Annals of Biomedical Engineering (© 2012)
DOI: 10.1007/s10439-012-0562-z

BMES BIOMEDICAL ENGINEERING SOCIETY™ www.bmes.org

Quantitative Analysis of Molecular Absorption into PDMS Microfluidic Channels

JACK D. WANG,[1] NICHOLAS J. DOUVILLE,[1] SHUICHI TAKAYAMA,[1,2] and MOHAMED ELSAYED[1,2]

[1]Department of Biomedical Engineering, University of Michigan, 1101 Beal Avenue, Ann Arbor, MI 48109, USA; and [2]Macromolecular Science and Engineering Program, University of Michigan, 1101 Beal Avenue, Ann Arbor, MI 48109, USA

(*Received 26 October 2011; accepted 27 March 2012*)

Associate Editor Sriram Neelamegham oversaw the review of this article.

Abstract—Microfluidic devices fabricated using poly(dimethylsiloxane) (PDMS) polymer are routinely used for *in vitro* cell culture for a wide range of cellular assays. These assays typically involve the incubation of cultured cells with a drug molecule or a fluorescent marker while monitoring a cellular response. The accuracy of these assays depends on achieving a consistent and reproducible concentration of solute molecules in solution. However, hydrophobic therapeutic and fluorescent molecules tend to diffuse into the PDMS walls of the microfluidic devices, which reduce their concentration in solution and consequently affect the accuracy and reliability of these assays. In this paper, we quantitatively investigate the relationship between the partition coefficient (log *P*) of a series of markers routinely used in *in vitro* cellular assays including [3H]-dexamethasone, [3H]-diazepam, [14C]-mannitol, [3H]-phenytoin, and rhodamine 6G and their absorption into PDMS microfluidic channels. Our results show that the absorption of a given solute into PDMS depends on the hydrophilic/hydrophobic balance defined by its log *P* value. Specifically, results demonstrate that molecules with log *P* less than 2.47 exhibit minimal absorption (<10%) into PDMS channels whereas molecules with log *P* larger than 2.62 exhibit extensive absorption (>90%) into PDMS channels. Further investigations showed that TiO_2 and glass coatings of PDMS channels reduced the absorption of hydrophobic molecules (log $P > 2.62$) by 2- and 4.5-folds, respectively.

Keywords—Log *P*, Microfluidic channels, PDMS, Molecular absorption.

INTRODUCTION

Microfluidic channels have been used in many biological applications including rapid high density sequencing,[40,56,67] polymerase chain reaction,[6,9,33,47,66] and detection of single molecules[11,16,19] since its development in the 1990s. They have been particularly useful in the development of biological assays such as particle immunoassays,[25] cell-based high throughput screening for drug discovery,[64] and capacitance cytometry of single eukaryotic cells.[58] The micron-scale size of these microfluidic devices offers many unique advantages including close mimicry of many *in vivo* microenvironments[23,38] and small volume requirement[49,62] compared to conventional analysis systems.

Several materials have been used to fabricate these microfluidic channels such as silicon,[7,8,55] ceramic,[51] quartz glass,[20,22,28,54] polymethyl methacrylate,[3,32] SU-8,[69] and poly(dimethylsiloxane) (PDMS).[14,44] The optical clarity,[30] biocompatibility,[60] and high oxygen diffusivity[13] of PDMS render it the most commonly used material in fabrication of microfluidic channels for biological applications. Several groups have capitalized on these advantages and used PDMS-based microfluidic channels to develop *in vitro* models of different physiological processes. For example, Sodunke *et al.* successfully conducted a study on the replication of hepatitis B virus in normal human hepatocytes using a PDMS-based microfluidic platform.[57] PDMS-based microfluidic channels also proved efficient in maintaining high and low density cultures of mammalian neuronal cells.[45] Recently, Huh *et al.* demonstrated the versatility of PDMS-based channels by creating a microfluidic airway system that simulates human airway epithelia and physiological airway flow found in the respiratory system.[29]

One key limitation of these channels is the hydrophobicity of the PDMS surface, which reduces its wettability by aqueous biological fluids and affects its

Address correspondence to Mohamed ElSayed, Department of Biomedical Engineering, University of Michigan, 1101 Beal Avenue, Ann Arbor, MI 48109, USA. Electronic mail: melsayed@umich.edu

Published online: 07 April 2012

compatibility with cell culture.[44] Plasma oxidation has been routinely used to introduce silanol groups on the PDMS surface to become more hydrophilic and fitting for *in vitro* cell culture.[44] However, diffusion of free uncross-linked PDMS chains from the bulk polymer to the channel surface diminishes its hydrophilic character causing the channel wall to gradually revert to its intrinsic hydrophobic nature.[18] Furthermore, exposure of oxidized PDMS surfaces to air for an extended period of time restores its hydrophobic character.[44] Extraction of PDMS surfaces using different solvents to remove unreacted oligomers followed by plasma oxidation was shown to increase the stability of hydrophilic PDMS surfaces by 7 days.[65] Combination of plasma oxidation followed by treatment with $SiCl_4$ and CCl_4 gases[5] or deposition of metal oxides[70] have also been used to increase the stability of hydrophilic PDMS surfaces. Despite the promise of these approaches in maintaining the hydrophilic nature of oxidized PDMS surfaces, they are not routinely used in fabrication of PDMS devices particularly those developed for biological assays. An earlier study confirmed the hydrophobicity of PDMS devices when Nile Red (a hydrophobic fluorescent dye) diffused into the PDMS wall of microfluidic channels shown by the retention of the fluorescence signal after repeated washes.[61] While this earlier study by Toepke *et al.* provides a visual evidence of molecular absorption into PDMS channels, it does not provide any quantitative methods to predict the absorption of other hydrophobic molecules into PDMS microfluidic channels.

In this report, we provide a quantitative correlation between the partition coefficient (log *P*) of a series of marker molecules and their absorption into microfluidic PDMS channels at pH 7.0 as a function of solution temperature (25 and 37 °C) and incubation time (0.5, 1, 2.5, and 4.5 h). The partition coefficient, log *P*, of a given molecule depends on its chemical structure and the associated hydrophilic/hydrophobic balance.[36] log *P* is experimentally determined by the ratio between molecule's concentration in a hydrophobic solvent (octanol) and concentration in a hydrophilic solvent (water) upon dissolution and reaching equilibrium in this biphasic solvent system as shown in Eq. (1).[36]

$$\log P = \log \frac{[\text{solute in octanol}]}{[\text{solute in water}]} \qquad (1)$$

Molecules with high log *P* value such as Nile Red (log $P = 5.0$)[34] are highly hydrophobic and can easily partition into lipid bilayers[24] and absorb into hydrophobic PDMS surfaces.[61] However, the majority of pharmaceutical and diagnostic agents have significantly lower log *P* values than 5 to achieve aqueous solubility and absorption from the gastrointestinal tract.[39] Consequently, there is a need to establish a relationship between log *P* of model solute molecules and their absorption into PDMS to predict the effect of molecular absorption of different therapeutic or diagnostic molecules on the accuracy and reproducibility of *in vitro* assays performed in microfluidic PDMS devices.

We selected five molecules with log *P* values that span the established log *P* range of current pharmaceutical agents[39,50] and are commonly used as markers to assess the viability and barrier properties of epithelial and endothelial monolayers (Fig. 1a). Mannitol is a hydrophilic small molecular weight molecule with six hydroxyl groups and a log *P* value of −3.10.[12] Mannitol permeates across epithelial and endothelial barriers through the aqueous pores in the tight junction complexes and is routinely used as a paracellular permeability marker.[15] Dexamethasone is a glucocorticoid with a potent anti-inflammatory effect.[53] Phenytoin is an anti-epileptic drug that is used to suppress abnormal brain activity including epileptic seizures.[27] Dexamethasone and phenytoin are moderately hydrophobic drug molecules with log *P* values of 1.83 and 2.47, respectively.[4,48] Both dexamethasone and phenytoin are substrates for the P-glycoprotein (P-gp) efflux pump present on the luminal side of intestinal epithelial cells, vascular endothelial cells, and cancer

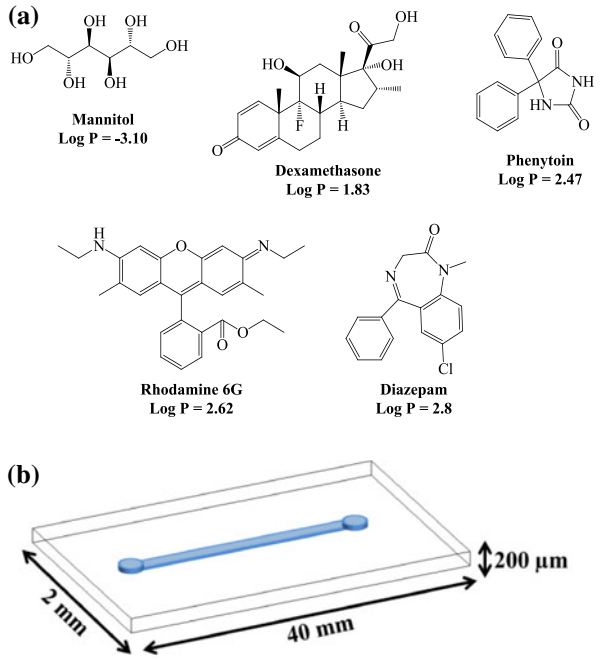

FIGURE 1. (a) Chemical structure and log *P* values of the selected marker molecules. (b) Schematic illustration of a single PDMS microfluidic channel.

cells.[2,63,68] Both molecules are routinely used to assess the functional expression of the P-gp efflux pump in epithelial and endothelial monolayers used as *in vitro* screening tools.[2,63] Rhodamine 6G is a hydrophobic, membrane-permeable, fluorescent dye with a log *P* of 2.62 that has been used to evaluate membrane potential based on its fluorescence intensity.[41] Diazepam is a hydrophobic drug molecule with log *P* of 2.8,[26] which allows it to freely diffuse across the cell membrane and is consequently used as a marker of transcellular permeability across epithelial and endothelial cell monolayers.[46] Diazepam is routinely used as a sedative, anticonvulsant, anxiolytic, and skeletal muscle relaxant.[42] These molecules were selected to span the log *P* range of major pharmaceutical agents (average log $P \sim 2.43$).[50] Furthermore, we evaluated the effect of TiO_2[52] and glass[1] coatings on the absorption of hydrophobic molecules into PDMS channels.

MATERIALS AND METHODS

Materials

Poly(dimethylsiloxane) (Sylgard 184) was purchased from Dow Corning (Midland, MI). SU-850 was purchased from MicroChem (Newton, MA). Titanium (IV) isopropoxide, tetraethyl orthosilicate (TEOS), and methyltriethyoxysilane (MTES) were purchased from Sigma Aldrich (St. Louis, MO). [14C]-D-mannitol (100 μCi/mL) and [3H]-phenytoin (1 mCi/mL) were purchased from Moravek Biochemicals and Radiochemicals (Brea, CA). [3H]-diazepam (1 mCi/mL) and [3H]-dexamethasone (1 mCi/mL) were purchased from American Radiolabeled Chemicals, Inc. (St. Louis, MO). Rhodamine 6G was purchased from Invitrogen (Carlsbad, CA). All chemicals were used as delivered without further purification.

Design and Fabrication of Microfluidic Channels

Microfluidic channels were fabricated using soft lithography following established procedures.[17] Briefly, PDMS prepolymer was mixed with the curing agent at a weight ratio of 10 (prepolymer):1 (curing agent) and was cast onto a 4 inches silicon wafer containing a 200 μm thick positive relief pattern. A single wafer was patterned to contain five evenly spaced microfluidic channels where each channel is 40 mm × 2 mm × 200 μm ($L \times W \times H$) (Fig. 1b). The PDMS layer and a solid PDMS slab with similar composition were cured overnight for 12 h at 60 °C. Access holes were punched with a 16 gauge blunt syringe (1.65 mm outer diameter) forming the inlet and outlet holes for each channel. PDMS prepolymer was used to bond the PDMS slab and channel upon exposure to plasma oxygen for 30 s. Prior to their use, fabricated PDMS channels were exposed to plasma oxygen for 5 min and immediately loaded with 15 μL of phosphate-buffered saline (PBS) solution.

Assessment of Markers Absorption

To measure the absorption of each molecule, 3 μL of [3H]-diazepam (2.67 μM), [14C]-D-mannitol (11.3 μM), or rhodamine 6G (52.2 μM) stock solutions were mixed with 12 μL of PBS and loaded into the PDMS channels. Given the high specific activity of [3H]-phenytoin (6.67 μM) and [3H]-dexamethasone (0.0076 μM), only 0.3 μL of the stock solution was mixed with 14.7 μL of PBS solution before loading into the PDMS channel. Loaded channels were incubated at 25 and 37 °C for 0.5, 1, 2.5, and 4.5 h. All concentrations are selected based on the minimum amount required for detection of these molecules in solution. The loaded marker solution was retrieved from each channel followed by washing the channel with 15 μL of fresh PBS for 12 consecutive times at different time points and immediately analyzed using liquid scintillation counting (Beckman LS 6500, Beckman Coulter Inc., Brea, CA) for radiolabeled markers or the Fluoroskan Ascent FL plate reader (Thermo Fisher Scientific Inc., Waltham, MA) for rhodamine 6G. The amount of each marker present in the collected washes was normalized to that initially loaded into each channel to determine percentage absorption of different markers. Absorption rate (%/min/cm^2) of each molecule was calculated by normalizing the percentage absorbed to the incubation time and channel surface area.

TiO_2 and Glass Coating of PDMS Channels

TiO_2 coating of PDMS channels was done following established protocols.[52] Briefly, PDMS microfluidic channels were filled with 2-propanol by applying a negative pressure of approximately 50 kPa at one end of the reservoirs while the remaining one was filled with 2-propanol. A mixture of 1:1 v/v of titanium (IV) isopropoxide and 2-propanol was prepared and pumped through the channel for 1 min to replace the loaded 2-propanol. The reservoirs were then allowed to dry in order to properly apply the TiO_2 coating to the surface of PDMS channels.

For glass coating, water (adjusted to pH 4.5 with HCl), TEOS, MTES, and ethanol were mixed at a 1:1:1:1 v/v to prepare the pre-conversion sol mixture following published procedures.[1] This solution was heated in a microwave oven for 15 s before incubating at 65 °C for 12 h. Channels were oxidized by oxygen plasma for 5 min to generate hydroxyl groups on the

PDMS surface to allow covalent coupling between PDMS and siloxanes. The channels were immediately filled with pre-converted sol mixture and placed on a hot plate at 100 °C for approximately 1 min to coat the channel surface. The sol solution was removed from the channel using a vacuum pump leaving the desired glass coating on the PDMS surface.

RESULTS AND DISCUSSION

Absorption of Mannitol in PDMS Microfluidic Channels

All channels used in the absorption experiments were fabricated using the same master. Channels were used 30–60 min after their plasma oxidation and they were easily loaded with PBS solution and remained intact throughout the absorption experiments. Channel consistency is maintained by using the same amount of PDMS for fabrication (50 g of PDMS prepolymer for five channels). All channels are then baked in the oven using the same master. Channel quality is checked by loading PBS solution and examined under the microscope at 10× magnification to confirm the absence of air bubbles. Microfluidic channels trapping any bubbles were immediately discarded.

Mannitol absorption into PDMS channels varied based on the incubation temperature and time (Fig. 2). The total amount of [14C]-mannitol retrieved from each channel in the initial collection (IC) and subsequent washes with fresh PBS were normalized to the amount of [14C]-mannitol loaded into the same channel and the difference represents the percentage of mannitol molecules absorbed into the PDMS surface (Fig. 2). Results show that 66–82% of the loaded mannitol was retrieved after incubation for 0.5–4.5 h in PDMS microfluidic channels at 25 °C (Fig. 2a). In comparison, 92–100% of the loaded mannitol was retrieved after incubation in similar microfluidic channels at 37 °C for the same incubation periods (Fig. 2b). Results show similar percentages of mannitol retrieval from PDMS channels at all incubation times regardless of the solution temperature (Figs. 2a and 2b). However, results show higher percentages of mannitol retrieval upon incubation at 37 °C compared to that observed at 25 °C, which is attributed to the formation of hydrogen bonds between the silanol's OH groups displayed on the surface of oxidized PDMS and the six hydroxyl groups of mannitol molecules at lower temperature. Elevating solution temperature from 25 to 37 °C provides sufficient energy to break the hydrogen bonds and increase mannitol retrieval at different time points (Fig. 2b).

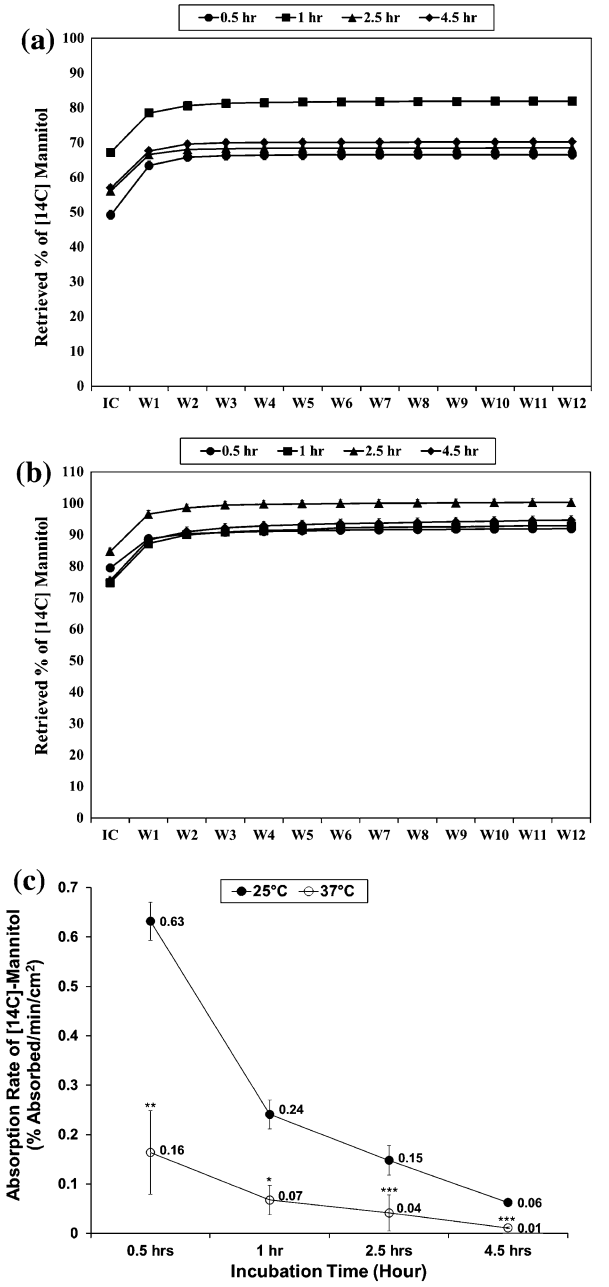

FIGURE 2. Cumulative amount of [14C]-mannitol retrieved in the initial collection (IC) and subsequent washes (W) normalized to the total amount of mannitol loaded into microfluidic PDMS channels incubated at (a) 25 °C and (b) 37 °C for 0.5 (●), 1.0 (■), 2.5 (▲), and 4.5 (♦) hours. (c) Absorption rate of [14C]-mannitol into PDMS microfluidic channels at 25 °C (●) and 37 °C (○) for 0.5, 1, 2.5, and 4.5 h. Results are the average ± the standard error of the mean collected from five different channels. Statistical difference in mannitol absorption rate as a function of solution temperature at a given incubation time point is identified by * when $p < 0.05$, ** when $p < 0.01$, and * when $p < 0.001$.**

We calculated the increase in solution energy due to temperature increase from 25 to 37 °C using the following heat capacity equation:

$$Q = \int_{T_1}^{T_2} C_p \, dT = C_p \times (T_2 - T_1) \quad (2)$$

where Q is the thermal energy resulting from the temperature difference, T_2 is the elevated temperature (37 °C), T_1 is the standard room temperature (25 °C), and C_p is the specific heat capacity for the mannitol solution, which is assumed to be equal to water (4.18 J g^{-1} K^{-1}) given that mannitol was dissolved in PBS. The calculated thermal energy as a result of temperature difference is 50.18 J g^{-1}.

Using the heat calculated in Eq. (2), we calculated the energy available from the elevated temperature to mannitol molecules (15 μL with density similar to water) loaded in the microfluidic channels using Eq. (3).

$$E_t = Q \times m \quad (3)$$

where E_t is the available energy and m is the mass of the mannitol solution. Based on Eq. (2), increasing the solution temperature from 25 to 37 °C provides 0.75 J of additional energy (E_t) to the loaded mannitol solution.

Earlier research showed that (O–H···O) hydrogen bond has 21 kJ mol^{-1} and requires a dissociation energy of 3.49×10^{-20} J.[21,43] Based on the specific activity of [14C]-D-mannitol (100 μCi/mL; 60×10^3 μCi/mmol), the number of mannitol molecules loaded in each microfluidic channel is 3.01×10^{15} molecules. These molecules will form 2.05×10^{16} hydrogen bonds and require 0.72×10^{-3} J to dissociate assuming that each of the OH groups of loaded mannitol molecules formed a hydrogen bond with a silanol group on the PDMS surface. Earlier calculations show that increasing the solution temperature from 25 to 37 °C provides 0.75 J, which is 1000-fold higher than the energy required to break the maximum number of hydrogen bonds formed between the loaded mannitol molecules and the OH groups displayed on the PDMS surface.

Absorption of mannitol and other molecules depend on the incubation time and the total surface area of PDMS microfluidic channels. Consequently, we normalized the percentage of absorbed molecules to the incubation period (minutes) and the PDMS surface area (cm^2) to calculate the absorption rate (%/min/cm^2) of different markers to extrapolate these findings to other microfluidic devices with different architectures and geometry. Results show that the absorption rate of mannitol dropped with the increase in incubation time and regardless of the incubation temperature, which indicates high absorption rate of mannitol molecules into the PDMS surface shortly after loading the channel (Fig. 2c). Mannitol absorption into PDMS channels clearly shows the effect of incubation temperature with a statistically higher absorption rate at 25 °C compared to that at 37 °C (Fig. 2c). Results show that mannitol ($\log P = -3.1$) exhibit low net absorption (<10%) and absorption rate (0.63%/min/cm^2) into microfluidic PDMS channels and can be used in different quantitative assays in PDMS microfluidic channels.

Absorption of Phenytoin and Dexamethasone in PDMS Microfluidic Channels

Phenytoin ($\log P = 2.47$) and dexamethasone ($\log P = 1.83$) are moderately hydrophobic drug molecules that are substrates for the P-gp efflux pump. Results show that absorption of phenytoin and dexamethasone into PDMS microfluidic channels increased with the increase in incubation time and solution temperature (Figs. 3 and 4). For instance, absorption of phenytoin increased from 8% (92% retrieved) to 22% (78% retrieved) of the loaded solute molecules after incubation for 0.5 and 4.5 h in PDMS channels at 25 °C, respectively (Fig. 3a). Phenytoin exhibited a similar absorption profile at 37 °C with 6 and 28% of the loaded solute molecules absorbed in the PDMS channel after incubation for 0.5 and 4.5 h, respectively (Fig. 3b). Results show that phenytoin's absorption rate at 37 °C was higher than that observed at 25 °C (Fig. 3c) except at 0.5 h, which can be attributed to the increase in solution thermal energy causing an increase in the kinetic energy of phenytoin molecules and their diffusivity into PDMS surface.[31]

Similarly, absorption of dexamethasone increased from 6% (94% retrieved) to 18% (82% retrieved) upon incubation in PDMS channels at 25 °C for 0.5 and 4.5 h, respectively (Fig. 4a). Dexamethasone exhibited a similar absorption profile at 37 °C with 2 and 30% of the loaded solute molecules absorbed in the PDMS channel after incubation for 0.5 and 4.5 h, respectively (Fig. 4b). Similar to phenytoin, results show that phenytoin's absorption rate at 37 °C was higher than that observed at 25 °C (Fig. 4c) except at 0.5 h. It also indicates continuous absorption of solute molecules into PDMS surface throughout the incubation period (Fig. 4c). These results collectively indicate that moderately hydrophobic molecules like phenytoin and dexamethasone can be used in quantitative assays in PDMS microfluidic devices with short analysis time (<0.5 h) when absorption of these solute molecules is insignificant.

Absorption of Rhodamine 6G and Diazepam in PDMS Microfluidic Channels

Rhodamine 6G ($\log P = 2.62$) and diazepam ($\log P = 2.8$) are highly hydrophobic drug molecules

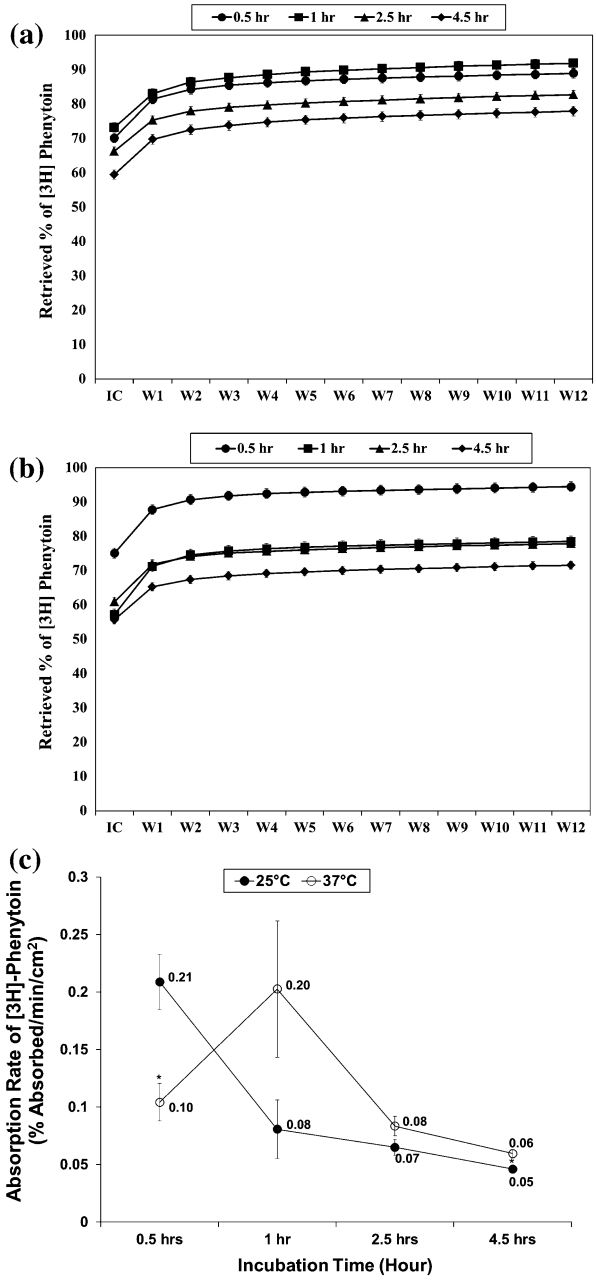

FIGURE 3. Cumulative amount of [3H]-phenytoin retrieved in the initial collection (IC) and subsequent washes (W) normalized to the total amount of phenytoin loaded into microfluidic PDMS channels incubated at (a) 25 °C and (b) 37 °C for 0.5 (●), 1.0 (■), 2.5 (▲), and 4.5 (♦) hours. (c) Absorption rate of [3H]-phenytoin into PDMS microfluidic channels at 25 °C (●) and 37 °C (○) for 0.5, 1, 2.5, and 4.5 h. Results are the average ± the standard error of the mean collected from five different channels. Statistical difference in phenytoin absorption rate as a function of solution temperature at a given incubation time point is identified by * when $p < 0.05$, ** when $p < 0.01$, and *** when $p < 0.001$.

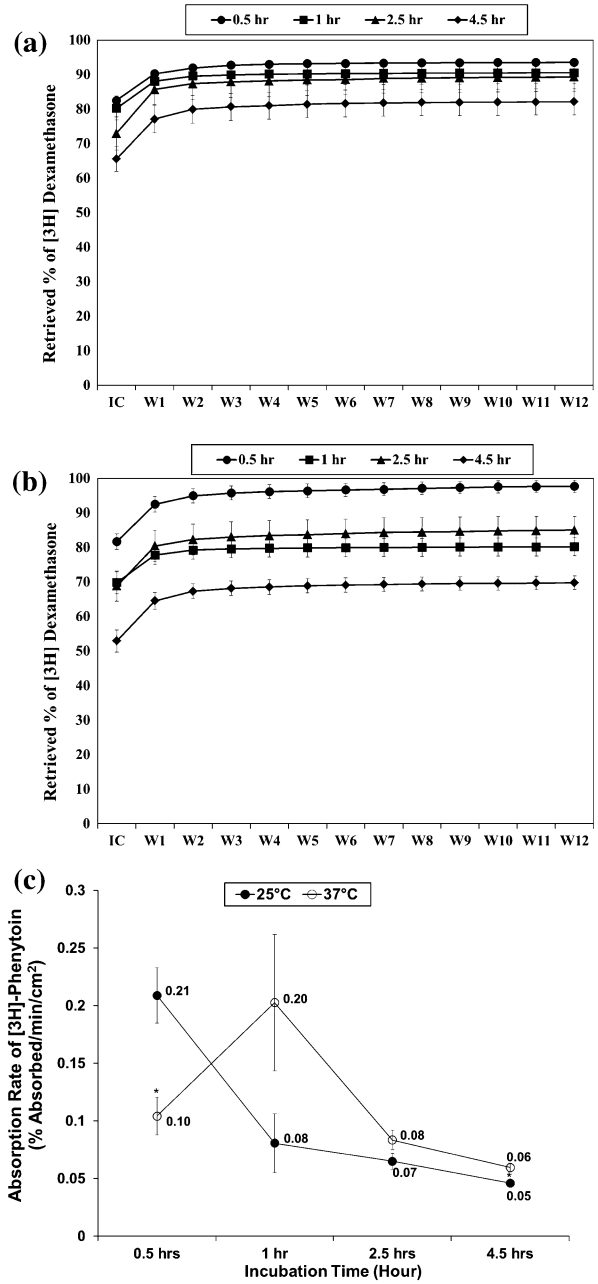

FIGURE 4. Cumulative amount of [3H]-dexamethasone retrieved in the initial collection (IC) and subsequent washes (W) normalized to the total amount of dexamethasone loaded into microfluidic PDMS channels incubated at (a) 25 °C and (b) 37 °C for 0.5 (●), 1.0 (■), 2.5 (▲), and 4.5 (♦) hours. (c) Absorption rate of [3H]-dexamethasone into PDMS microfluidic channels at 25 °C (●) and 37 °C (○) for 0.5, 1, 2.5, and 4.5 h. Results are the average ± the standard error of the mean collected from five different channels. Statistical difference in dexamethasone absorption rate as a function of solution temperature at a given incubation time point is identified by * when $p < 0.05$, ** when $p < 0.01$, and *** when $p < 0.001$.

that freely diffuse across the lipid bilayers of mammalian cell membranes and are routinely used to assess transcellular transport across epithelial and endothelial monolayers.[41,42,59] Results show that rhodamine 6G and diazepam exhibit extensive absorption into PDMS channels at 25 and 37 °C and all incubation time

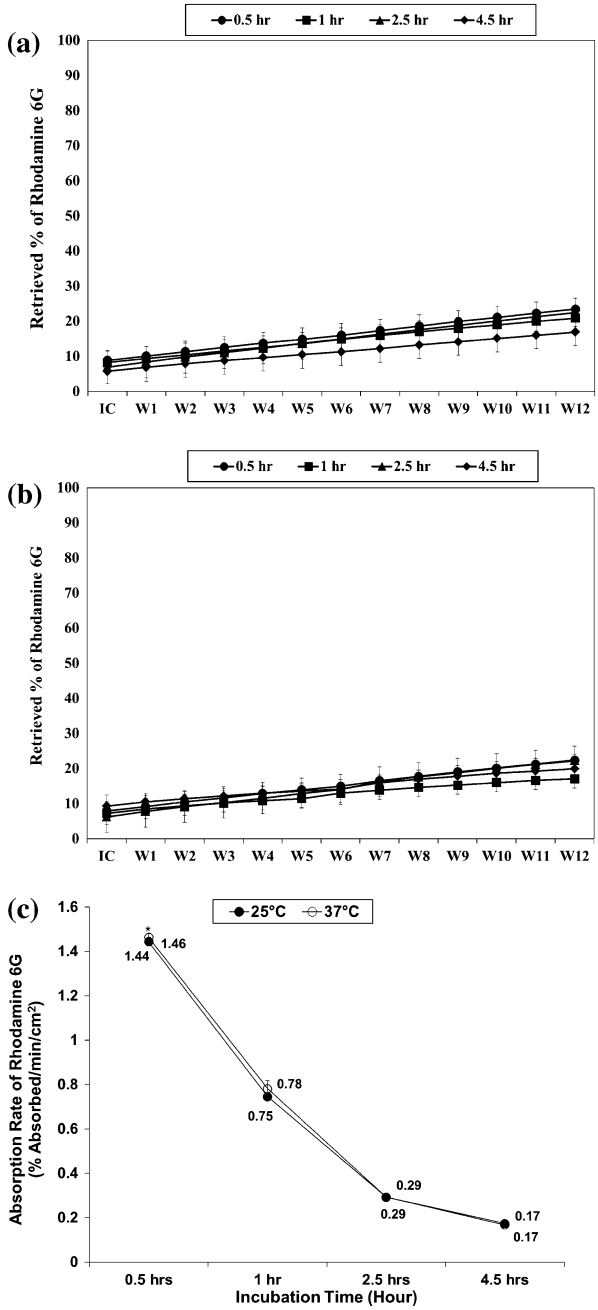

FIGURE 5. Cumulative amount of rhodamine 6G retrieved in the initial collection (IC) and subsequent washes (W) normalized to the total amount of rhodamine 6G loaded into microfluidic PDMS channels incubated at (a) 25 °C and (b) 37 °C for 0.5 (●), 1.0 (■), 2.5 (▲), and 4.5 (♦) hours. (c) Absorption rate of rhodamine 6G into PDMS microfluidic channels at 25 °C (●) and 37 °C (○) for 0.5, 1, 2.5, and 4.5 h. Results are the average ± the standard error of the mean collected from five different channels. Statistical difference in rhodamine 6G absorption rate as a function of solution temperature at a given incubation time point is identified by * when $p < 0.05$, ** when $p < 0.01$, and * when $p < 0.001$.**

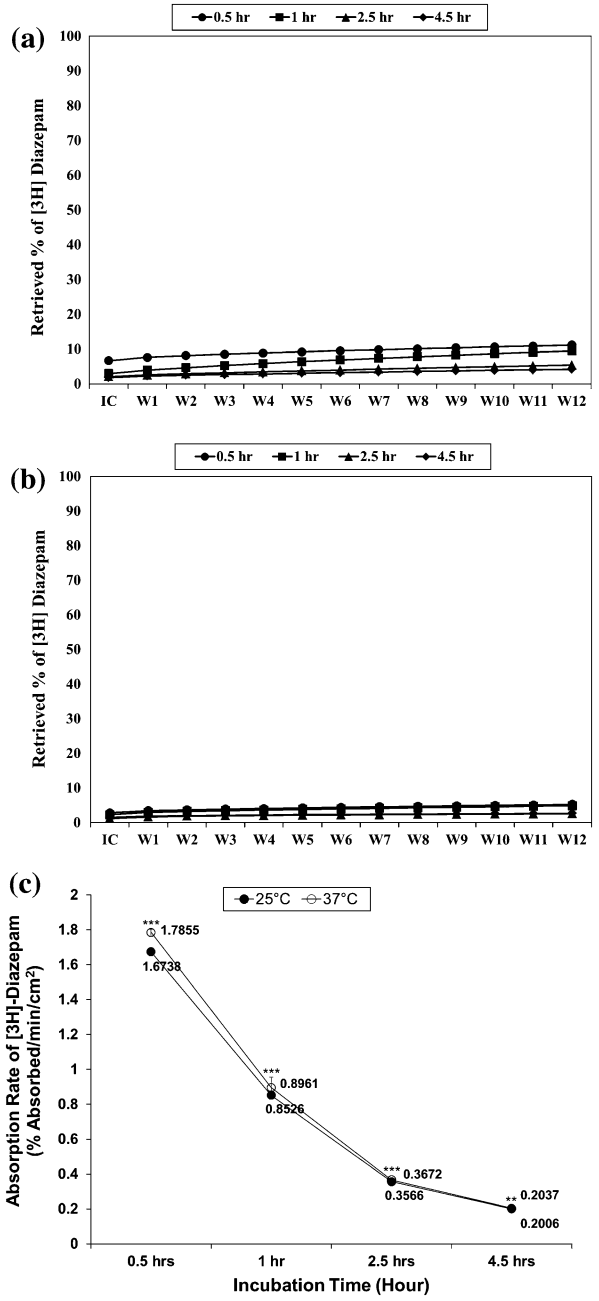

FIGURE 6. The cumulative amount of [3H]-diazepam retrieved in the initial collection (IC) and subsequent washes (W) normalized to the total amount of diazepam loaded into microfluidic PDMS channels incubated at (a) 25 °C and (b) 37 °C for 0.5 (●), 1.0 (■), 2.5 (▲), and 4.5 (♦) hours. (c) Absorption rate of [3H]-diazepam into PDMS microfluidic channels at 25 °C (●) and 37 °C (○) for 0.5, 1, 2.5, and 4.5 h. Results are the average ± the standard error of the mean collected from five different channels. Statistical difference in diazepam absorption rate as a function of solution temperature at a given incubation time point is identified by * when $p < 0.05$, ** when $p < 0.01$, and * when $p < 0.001$.**

points (Figs. 5 and 6). For example, 77 and 80% of the loaded rhodamine 6G molecules were absorbed in PDMS channels regardless of the incubation time at 25 and 37 °C, respectively (Figs. 5a and 5b). This is further emphasized in Fig. 5c showing the high absorption rate of 1.44%/min/cm^2 at 25 °C and

1.46%/min/cm^2 at 37 °C of rhodamine 6G upon incubation in PDMS channels for 0.5 h. Similarly, 90 and 95% of the loaded diazepam molecules absorbed into PDMS channels upon incubation at 25 and 37 °C, respectively (Figs. 6a and 6b). Results show that diazepam absorption into PDMS increased with the increase in incubation temperature shown by the significant increase in diazepam's absorption rate from 1.67%/min/cm^2 at 25 °C to 1.79%/min/cm^2 at 37 °C upon incubation for 0.5 h (Fig. 6c). These results clearly indicate that rhodamine 6G and diazepam exhibit rapid and extensive absorption into PDMS microfluidic channels, which will reduce the effective concentration of solute molecules present in solution and may influence the accuracy of different *in vitro* assays utilizing these markers.

Correlation Between Log P and Absorption in PDMS Microfluidic Channels

The partition coefficient, log *P*, of a given molecule depends on the hydrophilic/hydrophobic balance, which is dictated by its chemical structure. This report describes the absorption of a series of markers with different degrees of hydrophobicity reflected by their log *P* values, which span the log *P* range of the majority of therapeutic and diagnostic agents.[39,50] Correlating the log *P* of different markers with their absorption profile will allow the prediction of absorption of therapeutic molecules in PDMS microfluidic devices as a function of incubation time and solution temperature. Results show that mannitol exhibited the lowest absorption (95% retrieval) in PDMS channels upon incubation for 0.5 h at 37 °C, which is not surprising given its hydrophilic nature (log $P = -3.1$) (Fig. 7a). Dexamethasone (log $P = 1.83$) and phenytoin (log $P = 2.47$) also exhibited low absorption (>90% retrieval) into PDMS channels upon incubation for 0.5 h at 37 °C. In comparison, increasing the log *P* of investigated molecules to 2.62 (rhodamine 6G) and 2.8 (diazepam) led to a substantial increase in molecular absorption in PDMS channels under the same experimental conditions.

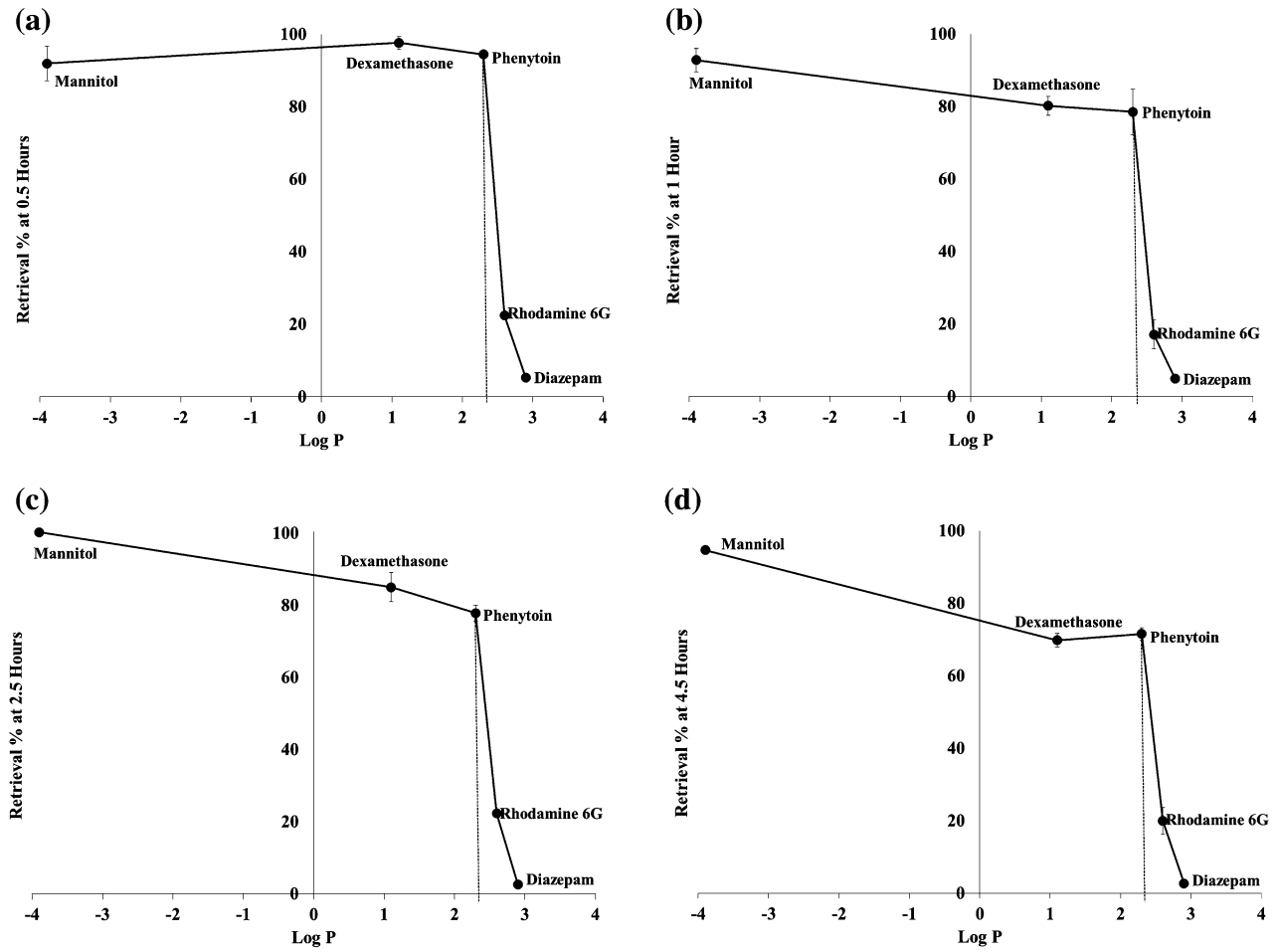

FIGURE 7. The relationship between the retrieved percentage of each marker molecules and its log *P* value after incubation in microfluidic PDMS channels for (a) 0.5, (b) 1.0, (c) 2.5, and (d) 4.5 h at 37 °C. Results are the average ± the standard error of the mean collected from five different channels.

These results suggest that there is a log P "threshold" between 2.47 and 2.62 where molecules with log $P <$ 2.47 exhibit minimal absorption into PDMS surfaces whereas those with log $P > 2.62$ get extensively absorbed into PDMS channels.

To better elucidate the difference in markers hydrophobicity, we used log P values to calculate the concentration of different marker molecules in octanol (Eq. (1)) and normalized the concentration of each marker in this organic layer to that of mannitol. Results show that the calculated concentration of dexamethasone, phenytoin, rhodamine 6G, and diazepam is ~85,000-, 372,000-, 525,000-, and 794,000-folds the concentration of mannitol partitioning into the organic octanol layer, respectively, which clearly shows the significant difference in hydrophobicity of different molecules. Further, it shows the significant difference in hydrophobicity between phenytoin and rhodamine 6G despite the small difference in their log P values, which suggests that there is a log P "threshold" for extensive absorption into PDMS microfluidic devices. The relationship between log P of different markers and their observed absorption into PDMS microfluidic devices was consistent at all incubation time points up to 4.5 h (Fig. 7).

Our results are supported by earlier studies by Lee *et al.* who examined the compatibility of different aqueous and organic solvents with PDMS-based microfluidic devices by measuring the partition of multiple organic solutes between bulk PDMS and different organic solvents.[35] Results of this investigation showed that aqueous solutions of rhodamine B (log $P = 2.74$)[59] and fluorescein (log $P = -0.67$)[10] exhibited different absorption profiles into bulk PDMS.[35] Specifically, fluorescein was not absorbed into PDMS whereas 60% of rhodamine B molecules got absorbed into bulk PDMS under the same experimental conditions.[35] These earlier results are in agreement with our findings and support the notion that absorption into PDMS depends on the solute's log P value. It is important to note that an analysis of over 3000 drug candidates between 1960 and 2000 showed that the mean log P value for these therapeutic molecules is approximately 2.43,[50] which is similar to the log P threshold identified in this report. This suggests that approximately 50% of current drugs can be used in different *in vitro* assays that utilize microfluidic PDMS devices without exhibiting appreciable absorption into PDMS surface. However, drugs with log P values >2.62 should be carefully evaluated before using them in any quantitative assays that utilize PDMS devices to eliminate the effect of their absorption into PDMS wall on the accuracy of the results.

Effect of TiO_2 and Glass Coating on Absorption in PDMS Channels

Culbertson and Weitz groups showed that TiO_2 and glass coatings prevent the diffusion of rhodamine B (log $P = 2.74$)[59] into the PDMS walls of microfluidic channels. This was indicated by the localization of the fluorescence signal to lumen of the channel compared to uncoated channels, which showed extensive fluorescence staining of the PDMS walls.[26,46] Earlier studies showed that the contact angle for uncoated Sylgard 184 PDMS is 110°, which indicates the high hydrophobicity of the PDMS surface.[52] However, TiO_2- and glass-coated PDMS channels have a significantly lower contact angle of 61° and 35°, respectively.[37,52] Consequently, we evaluated the effect of TiO_2 and glass coatings on diazepam (log $P = 2.8$) absorption into microfluidic PDMS channels upon incubation for 0.5 h at 37 °C (Fig. 8). Results show that the percentage of retrieved diazepam increased

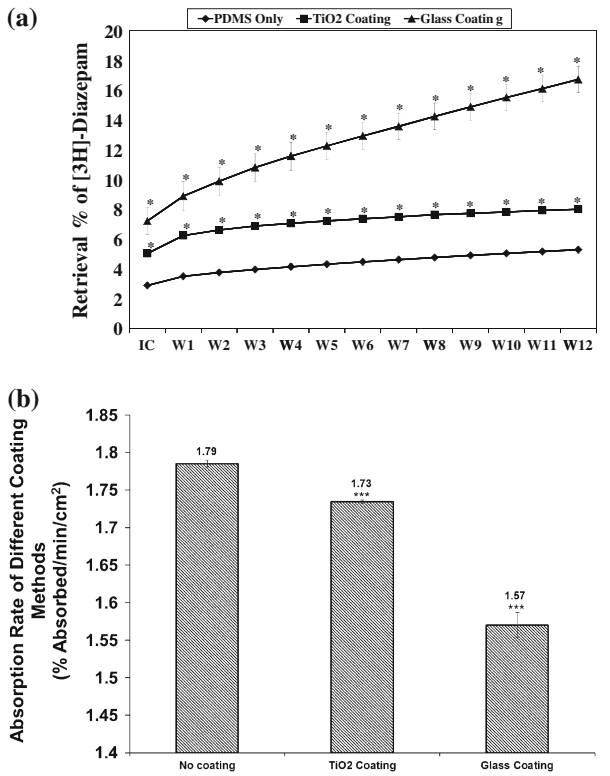

FIGURE 8. (a) Cumulative amount of [3H]-diazepam retrieved in the initial collection (IC) and subsequent washes (W) normalized to the total amount of diazepam loaded into uncoated (♦), TiO_2-coated (■), and glass-coated (▲) microfluidic PDMS channels for 0.5 h at 37 °C. (b) Absorption rate of [3H]-diazepam into uncoated and TiO_2- and glass-coated PDMS microfluidic channels upon incubation for 0.5 h at 37 °C. Results are the average ± the standard error of the mean collected from five different channels. Statistical difference in diazepam absorption rate as a function of channel coating is identified by * when $p < 0.05$, ** when $p < 0.01$, and * when $p < 0.001$.**

from 4% for uncoated PDMS channels to 8 and 18% in TiO_2- and glass-coated channels, respectively (Fig. 8a). Therefore, diazepam absorption rate decreased significantly from 1.79%/min/cm^2 for uncoated PDMS channels to 1.73%/min/cm^2 and 1.57%/min/cm^2 in TiO_2- and glass-coated channels, respectively (Fig. 8b). However, the decrease in diazepam absorption in TiO_2- and glass-coated channels did not match the low absorption rate of marker molecules with $\log P < 2.47$. These results suggest the potential of TiO_2 and glass coatings in reducing the absorption of hydrophobic molecules ($\log P > 2.62$) but coating conditions (e.g., number and thickness of coating layers) need to be further optimized to inhibit molecular absorption into microfluidic PDMS channels.

CONCLUSIONS

Our results provide a quantitative correlation between the $\log P$ of a series of markers and their absorption in microfluidic PDMS channels as a function of incubation time and temperature. Results show molecules with $\log P < 2.47$ exhibit minimal absorption (<10%) into PDMS channels whereas molecules with $\log P > 2.62$ exhibit extensive absorption in the same channels. Further, TiO_2 and glass coatings reduce the absorption of [3H]-diazepam ($\log P = 2.8$) in microfluidic PDMS channels. However, reduction in diazepam absorption to match the low levels observed with hydrophilic molecules ($\log P < 2.47$) requires a systemic investigation of the effect of coating parameters on net molecular absorption. These results clearly show the significance of considering the $\log P$ of different solute molecules before using them in quantitative assays in microfluidic PDMS devices.

REFERENCES

[1]Abate, A. R., D. Lee, T. Do, C. Holtze, and D. A. Weitz. Glass coating for PDMS microfluidic channels by sol-gel methods. *Lab Chip* 8:516–518, 2008.

[2]Baltes, S., A. M. Gastens, M. Fedrowitz, H. Potschka, V. Kaever, and W. Loscher. Differences in the transport of the antiepileptic drugs phenytoin, levetiracetam and carbamazepine by human and mouse P-glycoprotein. *Neuropharmacology* 52:333–346, 2007.

[3]Becker, H., and C. Gartner. Polymer microfabrication methods for microfluidic analytical applications. *Electrophoresis* 21(1):12–26, 2000.

[4]Bereczki, A., A. Tolokan, G. Horvai, V. Horvath, F. Lanza, A. J. Hall, and B. Sellergren. Determination of phenytoin in plasma by molecularly imprinted solid-phase extraction. *J. Chromatogr. A* 930:31–38, 2001.

[5]Bodas, D., and C. Khan-Malek. Formation of more stable hydrophilic surfaces of PDMS by plasma and chemical treatments. *Microelectron. Eng.* 83(4–9):1277–1279, 2006.

[6]Burns, M. A., B. N. Johnson, S. N. Brahmasandra, K. Handique, J. R. Webster, M. Krishnan, T. S. Sammarco, P. M. Man, D. Jones, D. Heldsinger, C. H. Mastrangelo, and D. T. Burke. An integrated nanoliter DNA analysis device. *Science* 282:484–487, 1998.

[7]Cheng, J., M. A. Shoffner, G. E. Hvichia, L. J. Kricka, and P. Wilding. Chip PCR. II. Investigation of different PCR amplification systems in microfabricated silicon-glass chips. *Nucleic Acids Res.* 24(2):380–385, 1996.

[8]Cheng, J., M. A. Shoffner, K. R. Mitchelson, L. J. Kricka, and P. Wilding. Analysis of ligase chain reaction products amplified in a silicon-glass chip using capillary electrophoresis. *J. Chromatogr. A* 732(1):151–158, 1996.

[9]Cheng, J., L. C. Waters, P. Fortina, G. Hvichia, S. C. Jacobson, J. M. Ramsey, L. J. Kricka, and P. Wilding. Degenerate oligonucleotide rpimed-PCR and capillary electrophoretic analysis of human DNA on microchip-based devices. *Anal. Biochem.* 257:101–106, 1998.

[10]Cheruvu, N. P. S., S. P. Ayalasomayajula, and U. B. Kompella. Retinal delivery of sodium fluorescein, budesonide & celecoxib following subconjunctival injection. *Drug Dev. Deliv.* 3(6), 2003.

[11]Chou, H. P., C. Spence, A. Scherer, and S. Quake. A microfabricated device for sizing and sorting DNA molecules. *Proc. Natl. Acad. Sci. USA* 96(1):11–13, 1999.

[12]Collett, A., N. B. Higgs, E. Sims, M. Rowland, and G. Warhurst. Modulation of the permeability of H_2 receptor antagonists cimetidine and ranitidine by P-glycoprotein in rat intestine and the human colonic cell line caco-2. *J. Pharmacol. Exp. Ther.* 288(1):171–178, 1999.

[13]Cox, M. E., and B. Dunn. Oxygen diffusion in poly (dimethyl siloxane) using fluorescence quenching. I. Measurement technique and analysis. *J. Polym. Sci. A* 24:621–636, 1986.

[14]de Jong, J., R. G. H. Lammertink, and M. Wessling. Membranes and microfluidics: a review. *Lab Chip* 6:1125–1139, 2006.

[15]Deli, M. A., C. S. Abraham, Y. Kataoka, and M. Niwa. Permeability studies on in vitro blood-brain barrier models: physiology, pathology, and pharmacology. *Cell. Mol. Neurobiol.* 25(1):59–127, 2004.

[16]Dörre, K., S. Brakmann, M. Brinkmeier, K. T. Han, K. Riebeseel, P. Schwille, J. Stephan, T. Wetzel, M. Lapczyna, M. Stuke, R. Bader, M. Hinz, H. Seliger, J. Holm, M. Eigen, and R. Rigler. Techniques for single molecule sequencing. *Bioimaging* 5:139–152, 1997.

[17]Duffy, D. C., J. C. McDonald, O. J. A. Schueller, and G. M. Whitesides. Rapid prototyping of microfluidic systems in poly(dimethylsiloxane). *Anal. Chem.* 70:4974–4984, 1998.

[18]Eddington, D. T., J. P. Puccinelli, and D. J. Beebe. Thermal aging and reduced hydrophobic recovery of polydimethylsiloxane. *Sens. Actuators B* 114:170–172, 2006.

[19]Effenhauser, C. S., G. J. M. Bruin, A. Paulus, and M. Ehrat. Integrated capillary electrophoresis on flexible silicone microdevices: analysis of DNA restriction fragments and detection of single DNA molecules on microchips. *Anal. Chem.* 69(17):3451–3457, 1997.

[20]Effenhauser, C. S., A. Manz, and H. M. Widmer. Glass chips for high-speed capillary electrophoresis separations with submicrometer plate heights. *Anal. Chem.* 65(19):2637–2642, 1993.

[21]Emsley, J. Very strong hydrogen bonds. *Chem. Soc. Rev.* 9:91–124, 1980.
[22]Fan, Z. H., and D. J. Harrison. Micromachining of capillary electrophoresis injectors and separators on glass chips and evaluation of flow at capillary intersections. *Anal. Chem.* 66(1):177–184, 1994.
[23]Fiddes, L. K., N. Raz, S. Srigunapalan, E. Tumarkan, and C. A. Simmons. A circular cross-section PDMS microfluidics system for replication of cardiovascular flow conditions. *Biomaterials* 31:3459–3464, 2010.
[24]Fowler, S. D., and P. Greenspan. Application of Nile red, a fluorescent hydrophobic probe, for the detection of neutral lipid deposits in tissue sections: comparison with oil red o. *J. Histochem. Cytochem.* 33(8):833–836, 1985.
[25]Han, J.-H., and J.-Y. Yoon. Reusable, polyethylene glycol-structured microfluidic channel for particle immunoassays. *J. Biol. Eng.* 3:6, 2009.
[26]Hansch, C., P. G. Sammes, and J. B. Taylor. Comprehensive Medicinal Chemistry: The Rational Design, Mechanistic Study & Therapeutic Applications of Chemical Compounds, Vol. 6. Oxford: Pergamon Press, 1990.
[27]Hardman, J. G., L. E. Limbird, and A. G. Gilman. Goodman & Gilman's the Pharmacological Basis of Therapeutics (10th ed.). New York: McGraw-Hill, 2001.
[28]Harrison, D. J., A. Manz, Z. Fan, H. Ludi, and H. M. Widmer. Capillary electrophoresis and sample injection systems integrated on a planar glass chip. *Anal. Chem.* 64(17):1926–1932, 1992.
[29]Huh, D., H. Fujioka, Y.-C. Tung, N. Futai, R. Paine, III, J. B. Grotberg, and S. Takayama. Acoustically detectable cellular-level lung injury induced by fluid mechanical stresses in microfluidic airway systems. *Proc. Natl. Acad. Sci. USA* 104(48):18886–18891, 2007.
[30]Huszank, R., S. Z. Szilasi, I. Rajta, and A. Csik. Fabrication of optical devices in poly(dimethylsiloxane) by proton microbeam. *Opt. Commun.* 283(1):176–180, 2009.
[31]Kittel, C., and H. Kroemer. Thermal Physics (2nd ed.). San Francisco: W.H. Freeman Company, 1980.
[32]Ko, J. S., H. C. Yoon, H. Yang, H.-B. Pyo, K. H. Chung, S. J. Kim, and Y. T. Kim. A polymer-based microfluidic device for immunosensing biochips. *Lab Chip* 3(2):106–113, 2003.
[33]Kopp, M. U., A. J. de Mello, and A. Manz. Chemical amplification: continuous-flow PCR on a chip. *Science* 280(5366):1046–1048, 1998.
[34]Kuchler, S., M. Abdel-Mottaleb, A. Lamprecht, M. R. Radowski, R. Haag, and M. Schafer-Korting. Influence of nanocarrier type and size on skin delivery of hydrophilic agents. *Int. J. Pharm.* 377:169–172, 2009.
[35]Lee, J. N., C. Park, and G. M. Whitesides. Solvent compatibility of poly(dimethylsiloxane)-based microfluidic devices. *Anal. Chem.* 75:6544–6554, 2003.
[36]Leo, A., C. Hansch, and D. Elkins. Partition coefficients and their uses. *Chem. Rev.* 71(6):525–616, 1971.
[37]Li, M., and D. P. Kim. Silicate glass coated microchannels through a phase conversion process for glass-like electrokinetic performance. *Lab Chip* 11:1126–1131, 2011.
[38]Lima, R., S. Wada, S. Tanaka, M. Takeda, T. Ishikawa, K.-i. Tsubota, Y. Imai, and T. Yamaguchi. In vitro blood flow in a rectangular PDMS microchannel: experimental observations using a confocal micro-PIV system. *Biomed. Microdevices* 10:153–167, 2008.
[39]Lipinski, C. A., F. Lombardo, B. W. Dominy, and P. J. Feeney. Experimental and computational approaches to estimate solubility and permeability in drug discovery and development settings. *Adv. Drug Deliv. Rev.* 46:3–26, 2001.
[40]Liu, S., Y. Shi, W. W. Ja, and R. A. Mathies. Optimization of high-speed DNA sequencing on microfabricated capillary electrophoresis channels. *Anal. Chem.* 71:566–573, 1999.
[41]Mandala, M., G. Serck-Hanssen, G. Martino, and K. B. Helle. The fluorescent cationic dye rhodamine 6G as a probe for membrane potential in bovine aortic endothelial cells. *Anal. Biochem.* 274:1–6, 1998.
[42]Mandrioli, R., L. Mercolini, and M. A. Raggi. Benzodiazepine metabolism: an analytical perspective. *Curr. Drug Metab.* 9(8):827–844, 2008.
[43]Markovitch, O., and N. Agmon. Structure and energetics of the hydronium hydration shells. *J. Phys. Chem. A* 111(12):2253–2256, 2007.
[44]McDonald, J. C., D. C. Duffy, J. R. Anderson, D. T. Chiu, H. Wu, O. J. A. Schueller, and G. M. Whitesides. Fabrication of microfluidic systems in poly(dimethylsiloxane). *Electrophoresis* 21:27–40, 2000.
[45]Millet, L. J., M. E. Stewart, J. V. Sweedler, R. G. Nuzzo, and M. U. Gillette. Microfluidic devices for culturing primary mammalian neurons at low densities. *Lab Chip* 7:987–994, 2007.
[46]Neuhaus, W., V. E. Plattner, M. Wirth, B. Germann, B. Lachmann, F. Gabor, and C. R. Noe. Validation of in vitro cell culture models of the blood-brain barrier: tightness characterization of two promising cell lines. *J. Pharm. Sci.* 97(12):5158–5175, 2008.
[47]Northrup, M. A., B. Benett, D. Hadley, P. Landre, S. Lehew, J. Richards, and P. Stratton. A miniature analytical instrument for nucleic acids based on micromachined silicon reaction chambers. *Anal. Chem.* 70:912–922, 1998.
[48]Paturi, J., H. D. Kim, B. Chakraborty, P. M. Friden, and A. K. Banga. Transdermal and intradermal iontophoretic delivery of dexamethasone sodium phosphate: quantification of the drug localized in skin. *J. Drug Target.* 18(2):134–140, 2010.
[49]Prakash, A. R., S. Adamia, V. Sieben, P. Pilarski, L. M. Pilarski, and C. J. Backhouse. Small volume PCR in PDMS biochips with integrated fluid control and vapour barrier. *Sens. Actuators B* 113:398–409, 2006.
[50]Proudfoot, J. R. The evolution of synthetic oral drug properties. *Bioorg. Med. Chem. Lett.* 15(4):1087–1090, 2005.
[51]Rebenklau, L., K.-J. Wolter, and S. Howitz. Realization of hybrid microfluidic systems using standard LTCC process. In: Electronic Components and Technology Conference. Las Vages, NV, 2000.
[52]Roman, G. T., and C. T. Culbertson. Surface engineering of poly(dimethylsiloxane) microfluidic devices using transition metal sol-gel chemistry. *Langmuir* 22:4445–4451, 2006.
[53]Schmelzeisen, R., and J.-C. Frolich. Prevention of postoperative swelling and pain by dexamethasone after operative removal of impacted third molar teeth. *Eur. J. Clin. Pharmacol.* 44:275–277, 1993.
[54]Seiler, K., D. J. Harrison, and A. Manz. Planar glass chips for capillary electrophoresis: repetitive sample injection, quantitation, and separation efficiency. *Anal. Chem.* 65(10):1481–1488, 1993.
[55]Shoffner, M. A., J. Cheng, G. E. Hvichia, L. J. Kricka, and P. Wilding. Chip PCR. I. Surface passivation of microfabricated silicon-glass chips for PCR. *Nucleic Acids Res.* 24(2):375–379, 1996.

[56]Simpson, P. C., D. Roach, A. T. Woolley, T. Thorsen, R. Johnston, G. F. Sensabaugh, and R. A. Mathies. High-throughput genetic analysis using microfabricated 96-sample capillary array electrophoresis microplates. *Proc. Natl. Acad. Sci. USA* 95(5):2256–2261, 1998.

[57]Sodunke, T. R., M. J. Bouchard, and H. M. Noh. Microfluidic platform for hepatitis B viral replication study. *Biomed. Microdevices* 10(3):393–402, 2007.

[58]Sohn, L. L., O. A. Saleh, G. R. Facer, A. J. Beavis, R. S. Allan, and D. A. Notterman. Capacitance cytometry: measuring biological cells one by one. *Proc. Natl. Acad. Sci. USA* 97(20):10687–10690, 2000.

[59]Tetko, I. V., J. Gasteiger, R. Todeschini, A. Mauri, D. Livingstone, P. Ertl, V. A. Palyulin, E. V. Radchenko, N. S. Zefirov, A. S. Makarenko, V. Y. Tanchuk, and V. V. Prokopenko. Virtual computational chemistry laboratory—design and description. *J. Comput. Aided Mol. Des.* 19:453–463, 2005.

[60]Thangawng, A. L., R. S. Ruoff, M. A. Swartz, and M. R. Glucksberg. An ultra-thin PDMS membrane as a bio/micro-nano interface: fabrication and characterization. *Biomed. Microdevices* 9(4):587–595, 2007.

[61]Toepke, M. W., and D. J. Beebe. PDMS absorption of small molecules and consequences in microfluidic applications. *Lab Chip* 6:1484–1486, 2006.

[62]Tung, Y.-C., Y.-s. Torisawa, N. Futai, and S. Takayama. Small volume low mechanical stress cytometry using computer-controlled Braille display microfluidics. *Lab Chip* 7:1497–1503, 2007.

[63]Ueda, K., N. Okamura, M. Hirai, Y. Tanigawara, T. Saeki, N. Kioka, T. Komano, and R. Hori. Human p-glycoprotein transports cortisol, aldosterone, and dexamethasone, but not progesterone. *J. Biol. Chem.* 267(34):24248–24252, 1992.

[64]Upadhyaya, S., and P. R. Selvaganapathy. Microfluidic devices for cell based high throughput screening. *Lab Chip* 10:341–348, 2010.

[65]Vickers, J. A., M. M. Caulum, and C. S. Henry. Generation of hydrophilic poly(dimethylsiloxane) for high-performance microchip electrophoresis. *Anal. Chem.* 78:7446–7452, 2006.

[66]Waters, L. C., S. C. Jacboson, N. Kroutchinina, Y. Khandurina, R. S. Foote, and J. M. Ramsey. Multiple sample PCR amplification and electrophoretic analysis on a microchip. *Anal. Chem.* 70:5172, 1998.

[67]Woolley, A. T., and R. A. Mathies. Ultra-high-speed DNA sequencing using capillary electrophoresis chips. *Anal. Chem.* 67:3676–3680, 1995.

[68]Yang, H.-w., H.-y. Liu, D.-m. Zhang, Y.-c. Liu, X.-d. Liu, G.-j. Wang, and L. Xie. Increased P-glycoprotein function and level after long-term exposure of four antiepileptic drugs to rat brain microvascular endothelial cells in vitro. *Neurosci. Lett.* 434(3):299–303, 2008.

[69]Zhang, J., K. L. Tan, G. D. Hong, L. J. Yang, and H. Q. Gong. Polymerization optimization of SU-8 photoresist and its applications in microfluidic systems and MEMS. *J. Micromech. Microeng.* 11(1):20–26, 2001.

[70]Zhou, J., A. V. Ellis, and N. H. Voelcker. Recent developments in PDMS surface modification for microfluidic devices. *Electrophoresis* 31:2–16, 2010.